



Material characterization of a pultrusion specific and highly reactive polyurethane resin system: Elastic modulus, rheology, and reaction kinetics

Onur Yuksel^{a, **}, Michael Sandberg^b, Ismet Baran^{a, *}, Nuri Ersoy^c, Jesper H. Hattel^b, Remko Akkerman^a

^a Faculty of Engineering Technology, University of Twente, NL-7500AE Enschede, the Netherlands

^b Department of Mechanical Engineering, Section of Manufacturing Engineering, Technical University of Denmark, Produktionstorvet Building 425, Kgs. Lyngby DK-2800, Denmark

^c Department of Mechanical Engineering, Bogazici University, Bebek, 34342, Istanbul, Turkey

ARTICLE INFO

Keywords:

A. Thermosetting resin
B. Cure behaviour
B. Rheological properties
B. Mechanical properties
E. Pultrusion

ABSTRACT

This study presents a detailed material characterization study of a pultrusion specific polyurethane resin system. Firstly, the chemical behaviour was characterized by utilizing differential scanning calorimetry. The cure kinetics was fitted well to an autocatalytic cure kinetics model with Arrhenius temperature dependency. The resin system did not show any inhibition time. Then, the viscosity evolution was observed using a rheometer. From these measurements, the gelation point was estimated from the criterion of cross-over point of storage and loss modulus curves. The corresponding cure degree of gelation point was found to be 0.79 using the cure kinetics model. The complex viscosity evolution through dynamic scans was predicted well with a cure degree and temperature dependent viscosity model. The elastic modulus and glass transition temperature of fully and partially cured samples were measured by means of DMA in tension mode. A five step cure hardening instantaneous linear elastic model was fitted well to a wide range of cure degree values after gelation. Lastly, the fitted material models were employed in a case study of a typical pultrusion process to visualize the effects of pulling speed on the material property evolution.

1. Introduction

Pultrusion is a continuous production technique of fiber reinforced composites in which different types of reinforcement such as continuous filament mats (CFM), fabrics, unidirectional and air texturised fibers can be used [1]. The increasing demand of lighter, stronger and cheaper products, have promoted the use of pultrusion processes in recent years. Due to its continuous nature and relatively high production rates, pultrusion is a popular process, especially for the manufacture of structural elements in the construction and infrastructure sectors [2]. In recent years, various improvements and modifications on the production technique are still implemented to increase the efficiency of the process [3–6]. Besides the practical improvements in the process, novel developments of pultrusion specific material systems have attracted wide interest. The main challenge of synthesizing better resin systems is the optimization of final product specifications and processability. The final product specifications should be sufficient in mechanical, thermal and

environmental aspects. The processability is essential to have higher output rate and better impregnation which require higher reactivity and lower viscosity, respectively.

During the pultrusion process, chemical and physical properties of the resin system evolve simultaneously. Local temperature gradients take place and, in particular, in relatively thick pultruded profiles due to the exothermic heat reaction of the thermosetting resin during curing. Such temperature gradient results in non-uniformity of curing shrinkage, mechanical properties, thermal expansion and contraction. Several experimental and numerical studies in the literature have been devoted to understand the direct link between process conditions and final properties. With numerical process models, it is possible to analyse the process limitations regarding the maximum pulling speed with respect to sufficient final cure degree or the required injection pressure to achieve a proper impregnation. The cure degree evolution in a pultrusion line was modelled using a cure kinetics model of the unsaturated polyester and epoxy [7]. The pressure field in a resin bath pultrusion die

* Corresponding author.

** Corresponding author.

E-mail addresses: o.yuksel@utwente.nl (O. Yuksel), i.baran@utwente.nl (I. Baran).

<https://doi.org/10.1016/j.compositesb.2020.108543>

Received 1 September 2020; Received in revised form 21 October 2020; Accepted 20 November 2020

Available online 5 December 2020

1359-8368/© 2020 The Authors. Published by Elsevier Ltd. This is an open access article under the CC BY license (<http://creativecommons.org/licenses/by/4.0/>).

was solved for various process parameters in a simplistic process model [8]. The flow in a resin injection pultrusion line was predicted in [9,10] using rheological properties and cure-kinetics of the resin system. A mechanical model was coupled with a thermochemical model in a novel framework to predict the residual stresses for various pultruded profiles [11]. The warpage in a hollow pultruded profile was predicted and experimentally validated in [12]. The spring-in value of an L-shaped profile consisting of different reinforcement types was successfully predicted in [13]. A detailed overview of numerical process models of pultrusion can be found in [14]. Apart from the cure kinetics and rheological properties, thermo-chemical mechanical (TCM) models require also the mechanical property evolution during the process to predict the residual stress formation. Therefore, a comprehensive material characterization study is essential to develop accurate numerical process models to capture the complex resin behaviour. With comprehensive constitutive material models, virtual experiments can be carried out to optimize the process parameters as well. The studies presented in [15,16] can be considered as comprehensive characterization studies for numerical process modelling. The authors characterized an epoxy resin system for resin transfer molding processes (RTM) in [15], and a pultrusion specific polyester resin in [16].

Among the alternatives of suitable material systems as polyesters and vinyl esters, polyurethanes (PU) are one of the most promising candidates to match the requirements for highly efficient pultrusion process [17]. PU resins are the only class of polymers showing thermoplastic, thermosetting or elastomeric behaviour depending on its structure [18], and the thermosetting type of PU is the most prominently used one in pultrusion. PU resins have versatile properties in terms of thermal, mechanical and chemical aspects. The comparison of the bending modulus and strength of the pultruded profiles in the transverse direction showed the superiority of PU based systems over other commonly used resin systems such as the unsaturated polyester, vinyl ester and epoxy [17]. Moreover, PU composites show better fatigue characteristics and damage resistance as compared to epoxy [18]. The thermal insulation capacity of a pultruded profile with a PU core was reported to have a considerable improvement with respect to the profiles with cork core [19]. In addition to its advantages regarding the above mentioned aspects, PU resins can also be synthesized with different vegetable oils or biomass residues to promote the replacement of petrochemical products with renewable or recycled materials [20–22]. Recycling of crosslinked polyurethane is also possible as reported in [23,24].

The chemical, chemorheological and mechanical properties of various type of polyurethanes have been intensively characterized in the literature. In [25], a model with two autocatalytic reactions was proposed to model the cure kinetics due to having double peak in differential scanning calorimetry (DSC) experiments. An inhibition time was also observed for this RTM specific resin system. Cure kinetics of an aliphatic elastomeric polyurethane system was fitted well to a Kamal-Sourour generalized autocatalytic equation and a model free iso-conversional equation in [26]. A model free approach was modified by the description of non-isothermal curing processes in [27]. A pultrusion specific polyurethane system was chemically characterized and the reaction of this system was shown to follow a second order cure rate equation in [28]. The chemorheological model developed by Kim and Macosko [29] has been commonly used for the viscosity evolution predictions of polyurethane systems through the process [30,31]. Dynamic mechanical properties of PU resins synthesized with different types of polyol and di-isocyanates etc. have been studied extensively [20,32]. A fully coupled thermal, chemorheological and mechanical constitutive material model is essential to predict the thermokinetics, cure behaviour, exothermic temperature peak, residual stresses and deformations during the pultrusion process. However, to the authors' knowledge, there exist no such model or characterization study of a pultrusion specific PU resin system in the current literature.

In the present paper, a comprehensive characterization study was performed on a two component isocyanate and polyol based PU resin

system. The methodology was developed to understand, describe and predict the evolution of thermo-chemorheological and mechanical material properties of a fast curing pultrusion specific PU resin system during the process. Using highly reactive resin in pultrusion increases the pulling speed which is mainly important to have higher production rates. However, the high reactivity of the resin generates some challenges for the characterization. Hence, a methodology to overcome these challenges is presented in this study. The exothermic heat reaction was measured and the cure kinetics parameters for the curing model were obtained utilizing a DSC. The cure degree and temperature dependent viscosity was modelled and the gelation point was determined using a rheometer. The elastic modulus and glass transition temperature (T_g) evolution of fully and partially cured specimens were captured by means of dynamical mechanical analysis (DMA) in tension mode. As a novel contribution to literature, cure kinetics, rheology, T_g evolution as well as cure degree and temperature dependent instantaneous storage modulus evolution of a pultrusion specific PU were obtained in an experimental framework and presented explicitly to be used in numerical process models. Finally, a case study on a typical pultrusion temperature profile was carried out to simulate the material property evolution through a pultrusion die.

2. Cure kinetics

The variation of differential heat flow as a function of temperature and time in DSC gives a quantitative information about the exo- or endothermic reactions. The curing process of a thermosetting resin is an exothermic reaction. In principle, a thermosetting resin system generates all of its potential heat from its zero degree of cure (DOC) state to the fully cured state which is denoted the total heat of exothermic reaction. With a known total heat of exothermic reaction, the DOC evolution through a thermal cycle is obtained by the integration of the generated heat measured by the use of DSC.

A 'Mettler Toledo DSC822e' DSC was used to obtain the cure characteristics of the investigated PU resin. One feature of this DSC equipment worth pointing out is that it allows the user to take the sample out or put it in during the tests. Therefore, to catch the first heat flow during a high temperature isothermal scan, the sample was inserted into the DSC after the test and data sampling were started. Especially for a fast curing resin, like the resin system characterized in this study, this capability was essential to limit losing data due to pre-curing [33].

The components in the batches of 40g of mixture with proper ratios were mixed for 40 s. The whole procedure of the sample preparation took around 2 min and 50 s. The sample preparation times can be considered as comparable to the industrial application, where the PU resin constituents are mixed by the static mixers before being injected to the impregnation chamber. On average 15mg of samples were encapsulated in aluminum DSC crucibles.

Both isothermal and dynamic DSC scans were carried out to investigate the cure kinetics. Dynamic scans were performed from 25 °C to 200 °C with a heating ramp of 5 °C/min, 7.5 °C/min and 10 °C/min. The total heat of reaction was calculated by integrating the area under heat flow curves of dynamic scans with respect to time. A baseline between the onset and the end of reaction for this integration was drawn as described in [15]. The isothermal measurements were performed at 70 °C, 90 °C, 110 °C, 120 °C, 130 °C. The evolution of DOC through the tests was obtained using the relation given in Eq. (1).

$$\alpha = \frac{1}{H_T} \int_0^t \left(\frac{dH}{dt} \right) dt \quad (1)$$

where α is the DOC, H_T is the total heat of reaction, H is the heat reaction and t is time.

Fig. 1 depicts the heat flow curves of isothermal DSC scans. The peaks in heat flow curves were observed before 20 s of test time which showed how reactive the resin system was. Moreover, there was no

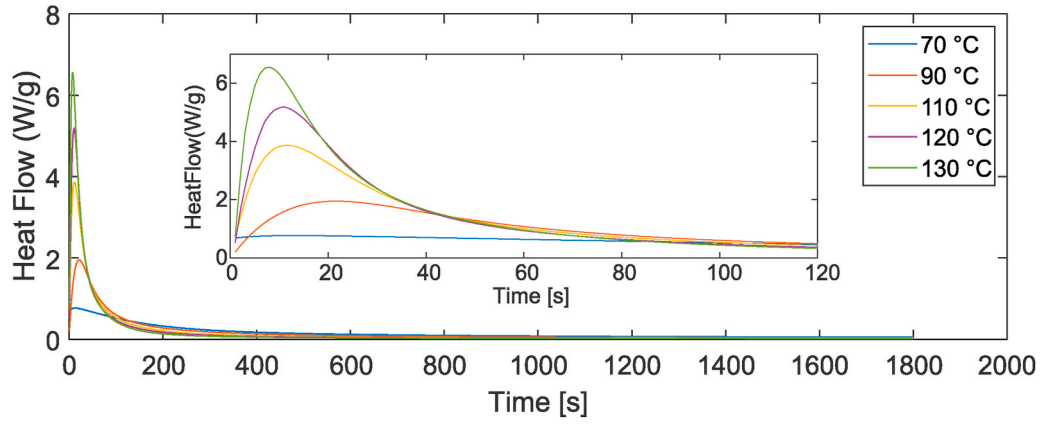


Fig. 1. The heat flow evolution in the isothermal DSC scans.

inhibition time observed during these tests because, when the PU sample was put in the DSC pan, the temperature of the pan was already at the testing temperature. In other words, the curing reaction started immediately at the studied isothermal DSC temperatures. It should be noted that there was no inhibitor mixed with the PU resin. The inhibition of the resin can be observed as it is cured at lower temperatures close to the room temperature which would not be a preferable case in pultrusion processes because ideally the resin should be cured in a short time within the die at elevated temperatures.

The total heat of reaction was needed to obtain the cure degree evolution through an isothermal DSC scan. The average total heat of reaction, which was calculated via the heat flow curves of dynamic scans, was found to be approximately 275 J/g with a standard deviation of 8.3 J/g. Similar polyurethane resin systems were reported to have 214 J/g and 280 J/g of total heat of reaction respectively in [28,34].

Due to lack of secondary peak and inhibition time for the studied DSC temperatures (70–130 °C), the cure rate was typically described by the following cure kinetics equation [35] that includes an Arrhenius type temperature dependency:

$$\frac{d\alpha}{dt} = A_0 \exp\left(\frac{-E_a}{RT}\right) \alpha^m (1 - \alpha)^n \quad (2)$$

where A_0 is a pre-exponential factor, E_a is the activation energy, and m, n are reaction orders, all obtainable by the DSC experiments. R is the gas constant and T is the absolute temperature.

The cure degree and cure rate as functions of time and temperature were taken from the measurements. The activation energy (E_a) was calculated from the slope of the relationship between inverse temperature ($1/T$) and natural logarithm of cure rate ($\ln(d\alpha/dt)$) at a low DOC

($\alpha = 0.1$ see Fig. 2 (a)). Here, $\alpha = 0.1$ was determined based on the work done in [15]. The other constants in the cure kinetics model (Eq. 2) were determined using a weighted least squares non-linear regression analysis. The DOC and cure rate evolution used in the regression analysis were derived from the isothermal DSC scans. Fig. 2(b) shows the fitting results for each isothermal temperature. It is seen that the temperature and degree of cure dependency of the cure rate was captured accurately with the cure kinetics model. The fitted parameters are listed in Table 1. Fig. 3 shows the measured and predicted DOC evolution. The results indicate that a reasonably good fit was obtained for the DOC evolution as a function of time for a temperature span from 70 °C to 130 °C. It is seen that the PU resin was approximately 80% cured within 160 s at 130 °C.

3. Chemorheology

Rheological tests of thermosetting resins provide valuable information about the physical transitions that occur during cure. This includes the temperature and cure degree dependent viscosity, as well as the liquid to rubbery transition at the gelation point. An ‘Anton Paar Physica MCR 501’ rheometer was used to measure the rheological properties of the material system. Out of alternative geometries as concentric cylinders (Couette flow), cone and plate etc., plate-plate geometry was chosen. The oscillatory tests were performed using 25 mm diameter

Table 1

The estimated cure kinetics parameters (Eq. (2)).

A_0 [1/s]	E_a [kJ/mol]	m	n
22648	41.2754	0.4899	3.1020

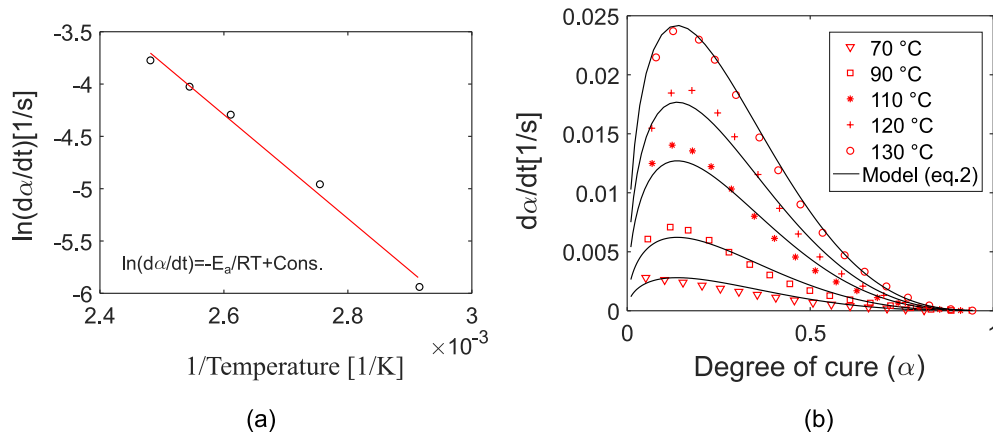


Fig. 2. The natural logarithm of cure rate as a function of inverse temperature (a), cure rate as a function of degree of cure (b).

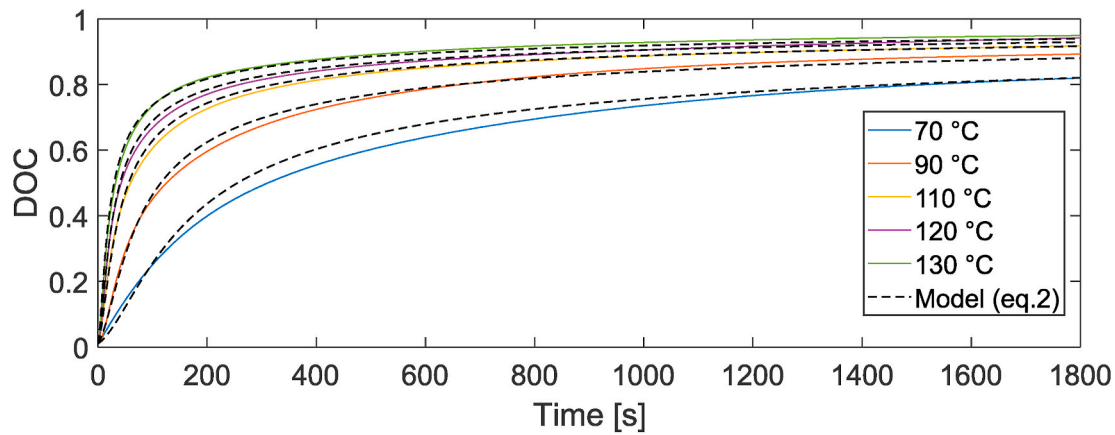


Fig. 3. The experimental and the predicted (best fit) cure degree evolution.

disposable aluminum plates with a 1 mm gap between the plates.

The mixing protocol for the rheological tests was the same as the mixing protocol of DSC samples. The preparation time was recorded for each rheometer test. The average preparation time before the initiation of tests was around 5 min. To avoid air entrapment and bubble formation during cure in the rheometer, components of the resin system were degassed separately for 30 min before mixing them for each test.

As discussed, the characterized resin system is highly reactive and does not show any inhibition time. Therefore, the rheological measurements were performed dynamically and started from the room temperature to prevent precure. The tests were started from 25 °C and performed up to 200 °C or when the complex viscosity reached a value of $10^4 \text{ Pa}\cdot\text{s}$. Three different heating rates of $2.5^\circ\text{C}/\text{min}$, $5^\circ\text{C}/\text{min}$ and $7.5^\circ\text{C}/\text{min}$ were applied to distinguish the effect of temperature and cure degree on the viscosity evolution. The tests were carried out in oscillatory mode at constant 1% strain amplitude and 1 Hz of frequency.

Another important material behaviour observed with a rheometer is the gelation. The gelation point has been determined with different approaches and criteria in the literature. The crossover point of storage modulus (G') and loss modulus (G'') was considered as a criterion of gelation point in [36]. The loss tangent cross-over at different frequencies was used in [37]. The moment when the viscosity was equal to a predetermined value was defined in [38] for the detection of the

gelation point. The cross-over of (G') and (G'') was chosen as the criterion for gelation point determination in this study. When (G') passes (G''), the material starts carrying mechanical loads which indicates the gelation.

Through the dynamic rheometry scans, the DOC evolution was obtained using the fitted cure kinetics model (Eq.2). Fig. 4 depicts the cross-over points of (G') and (G''). It is seen that the storage modulus value at the cross-over of (G') and (G'') decreased with a decrease in the heating ramp. More specifically, storage modulus values of approximately 15 kPa, 4 kPa and 2 kPa were obtained for the heating ramp of $2.5^\circ\text{C}/\text{min}$, $5^\circ\text{C}/\text{min}$ and $7.5^\circ\text{C}/\text{min}$, respectively. Fig. 5 represents the complex viscosity together with temperature and DOC evolutions up to the gelation point of each sample. It is seen that the required time to reach to the gelation point decreased with an increase in heating rate. The complex viscosity showed a sudden jump right before the gelation due to the increase in temperature. The obtained complex viscosity at the gelation was approximately $3000 \text{ Pa}\cdot\text{s}$, $780 \text{ Pa}\cdot\text{s}$ and $185 \text{ Pa}\cdot\text{s}$ for the heating rate of $2.5^\circ\text{C}/\text{min}$, $5^\circ\text{C}/\text{min}$ and $7.5^\circ\text{C}/\text{min}$, respectively. The higher heating ramps resulted in gelation at higher temperatures. The lower storage modulus and complex viscosity values at the gelation point for the higher heating ramps are related to temperature-softening. By using the cure kinetics model, the corresponding gelation cure degrees were determined as approximately 0.79, 0.78 and 0.75 for the

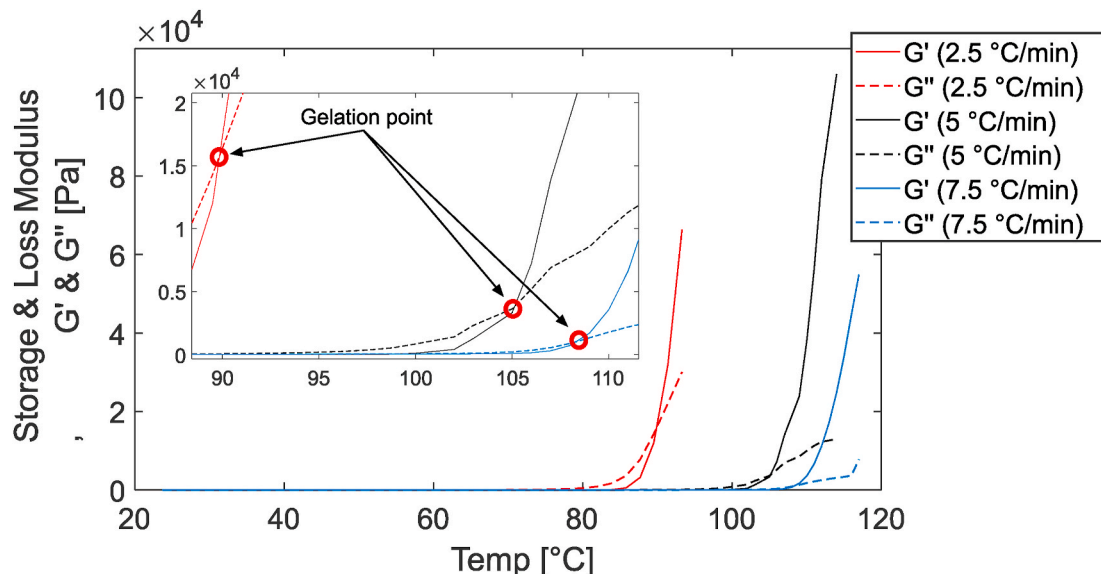


Fig. 4. The cross-over points of G' and G'' (gelation point).

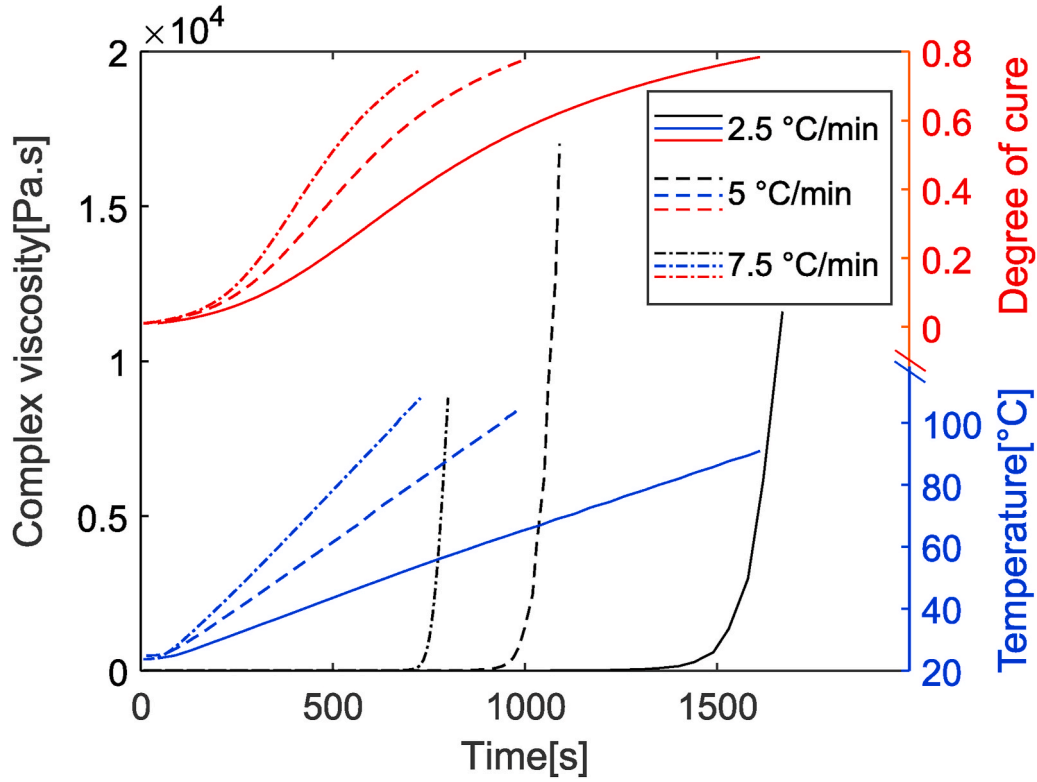


Fig. 5. The complex viscosity, degree of cure and temperature evolution as a function of time.

heating ramps of 2.5°C/min, 5°C/min and 7.5°C/min, respectively. It is seen that the gelation cure degrees were found to be very close to each other with a maximum of deviation of approximately 5% (0.79 versus 0.75) among different heating rates as expected. The slight deviation (5%) can be due to the inherent measurement errors as well as slight discrepancy between the cure kinetics model and the DSC measurements (see Figs. 2 and 3). The estimated DOC values at the gelation point were close enough to each other to reveal the accuracy of the fitted cure kinetics model.

The model, proposed by Kim and Macosko [29], was selected to characterize the viscosity evolution of the resin system (Eq. (3)).

$$\eta(T, \alpha) = \eta(T) \left(\frac{\alpha_g}{\alpha_g - \alpha} \right)^{(a+b\alpha)} \quad (3)$$

where α_g is the corresponding DOC for the gelation point. The DOC value used in Eq. (3) was estimated via the cure kinetics model (Eq. (2)) with respect to the temperature history of each test individually. In Eq. (3), a and b are the constants and $\eta(T)$ is the temperature dependent viscosity function which was defined as,

$$\eta(T) = \eta_0 \exp\left(\frac{E_{a,M}}{RT}\right) \quad (4)$$

where η_0 is the pre exponential factor, $E_{a,M}$ is the activation energy, R is the gas constant and T is the absolute temperature.

The DOC of the gelation point was estimated as 0.79, which is within the reported range of 0.65 – 0.85 provided in previous studies [31,39]. After the estimation of gelation point, the viscosity model (Eq. (3)) was fitted to the complex viscosity results for each heating ramp by utilizing a weighted least squares non-linear regression analysis with known DOC and temperature evolution. The obtained model parameters are listed in Table 2. Lower temperatures at gelation were obtained for lower heating rates because a longer time span to reach gelation was the case as seen in Fig. 6(a) and (b). It is seen that the viscosity evolution as a function of time, temperature and DOC was captured accurately using the fitted

Table 2

The estimated rheology model parameters (Eq. (3), Eq. (4)).

α_g	η_0 [Pa.s]	$E_{a,M}$ [kJ/mol]	a	b
0.79	$6.944 \cdot 10^{-5}$	24.274	0.016	3.094

model.

4. Cure degree and temperature dependent elastic modulus

The dynamical mechanical analysis is carried out to observe the temperature and frequency dependent mechanical behaviour of materials. Unlike quasi-static tests, dynamic loads can be exerted in a DMA. When applying a sinusoidal deformation, for example, the ratio between the stress and strain together with their time shift are used to characterize the storage and loss moduli of the material. These moduli can then be used to characterize the elastic and viscous behaviour of the material, respectively. The ratio between the loss and storage modulus is called the damping ratio which is equal to the phase angle (tan delta). The maximum tan delta through a temperature sweep is one of the most commonly used indicator of T_g .

DMA tests were carried out in a DMA ‘GABO Eplexor 2000 N’ with 50 N load cell. A fixture for tensile loading was employed for the tests. The temperature sweeps between 25°C and 200°C were carried out with 1 Hz frequency and 1°C/min heating ramp. Partially cured and fully cured pure resin specimens were tested to observe elastic modulus and T_g evolution with varying DOC.

To evacuate all bubbles (voids) from the specimens, the mixture was degassed in a vacuum chamber after mixing the components. The pure resin specimens were handled by casting the resin mixture between glass platens. A mould release agent was applied on the platens before casting and tacky tape was used as sealant between the platens. With suitable spacers, 4 mm thickness of pure PU plate was obtained. To have a vitrified resin, the degassed cast mixture was kept in an oven at 60°C for

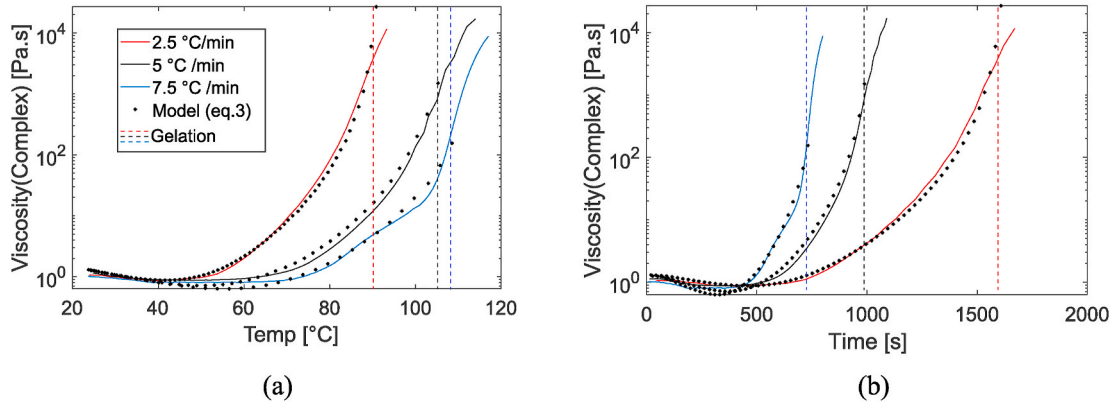


Fig. 6. The measured and predicted viscosity as a function of temperature (a) and time (b).

30 min. Specimens were cut out from the vitrified resin platen by utilizing a diamond saw with cooling water. After the preparation steps, specimens were dried in a vacuum oven at 40 °C and kept in a desiccator. Finally, the desired amount of post curing was performed on cut out specimens in an oven. One specimen was tested directly after vitrification. The other partially cured specimens were post-cured at 90 °C, 100 °C, 120 °C and 170 °C for 30 min. To check the residual cure reaction in the partially cured DMA samples, another DSC 'TA instrument DSC 2500' was utilized. Isothermal scans were performed at 170 °C to measure the residual cure and estimate the DOC of the partially cured DMA samples.

Measuring the elastic modulus evolution through a representative temperature and DOC range of the process is an arduous task due to phase change of the material. Below the corresponding DOC of gelation point, the resin is considered as liquid. Above the gelation point, the resin system is in rubbery state where the current temperature is higher than the glass transition temperature. In its glassy state, the current temperature is lower than the glass transition temperature. Simultaneously, T_g evolves through the process with increasing DOC. Therefore, capturing the T_g evolution throughout a process is required to predict the mechanical behaviour. There are different techniques to determine T_g in which a modulated DSC, thermal mechanical analysis (TMA), rheometer or DMA can be utilized. Tan delta peak measured with DMA was chosen as the indicator of T_g due to its direct association with the mechanical behaviour shift from glassy to rubbery state. T_g can also be defined as a function of DOC. DiBenedetto equation is the most commonly used expression [40,41], but different empirical equations have also been used to define the relation between T_g and DOC [42].

Fig. 7(a) shows the elastic modulus evolution of the samples with

various cure degrees. The tan delta evolution of these samples are shown in Fig. 7(b). Dashed lines indicate the tan delta peak of each sample which corresponds to T_g . The initial DOC of the partially cured samples at the beginning of the DMA tests were determined from the measured residual exothermic reactions of these samples utilizing DSC.

The investigated range of DOC for the elastic modulus evolution was relatively small due to the gelation point at 0.79 DOC. Therefore, the T_g evolution was modelled linearly as a function of DOC after the gelation point. The expression of T_g vs. α was derived from linear fitting of T_g and DOC values. These relations were captured via DMA and residual exothermic reaction, respectively. The relation between T_g and DOC was defined as " $T_g(\alpha) = -321.5 + 469.4 \cdot \alpha$ ". The fitted relation between DOC and T_g is shown in Fig. 8.

The time dependent elastic modulus evolution as a function of cure degree was modelled with a cure hardening instantaneous linear elastic (CHILE) model [35]. A five step partial function as shown in Eq. (5) was chosen in order to fit better to the elastic modulus evolution of the fully and partially cured samples. The proposed temperature and cure dependent elastic modulus in Eq. (5) was determined based on the initial trials performed for the DMA analysis of the PU resin.

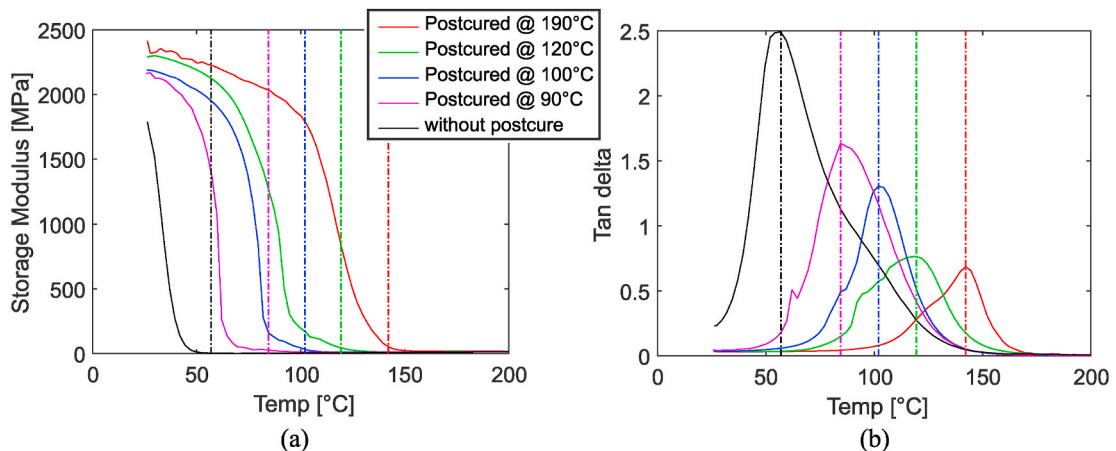


Fig. 7. Elastic moduli(a) and tan delta evolution (b) of partially and fully cured specimens.

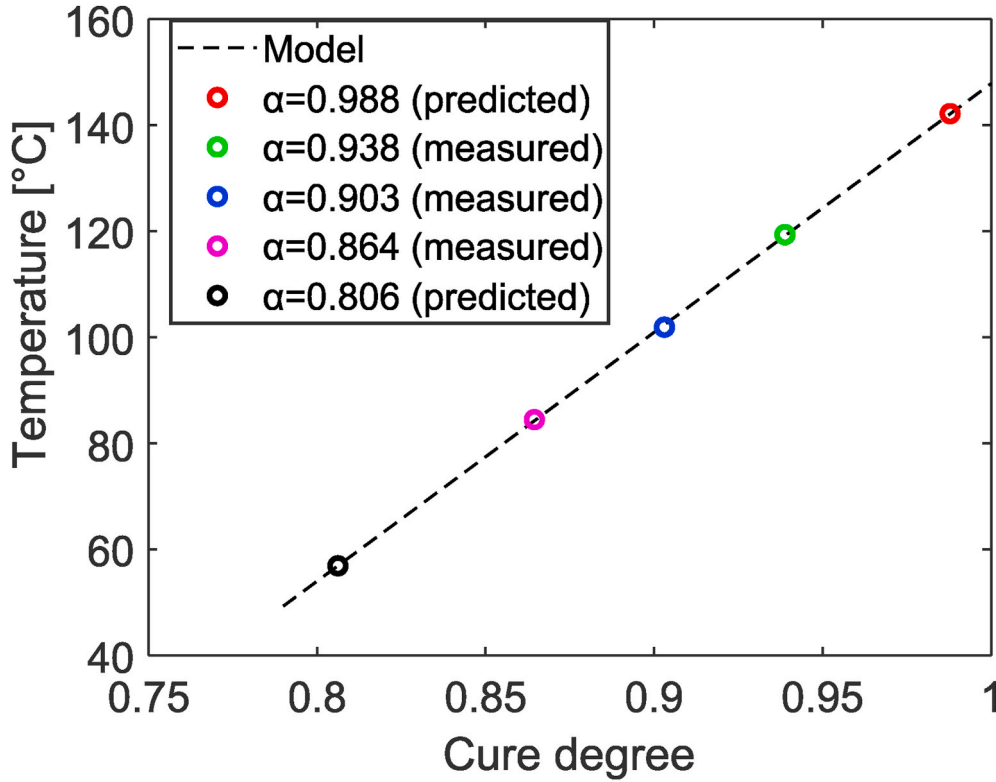


Fig. 8. The glass transition temperature evolution as a function of cure degree.

$$E_r = \begin{cases} E_r^1, & T^* \leq T_{C1} \\ E_r^2 + \frac{T^* - T_{C2}}{T_{C1} - T_{C2}} (E_r^1 - E_r^2), & T_{C1} < T^* \leq T_{C2} \\ E_r^3 + \frac{T^* - T_{C3}}{T_{C2} - T_{C3}} (E_r^2 - E_r^3), & T_{C2} < T^* \leq T_{C3} \\ E_r^4 + \frac{T^* - T_{C4}}{T_{C3} - T_{C4}} (E_r^3 - E_r^4), & T_{C3} < T^* \leq T_{C4} \\ A_e \exp(-K_e T^*), & T_{C4} < T^* \leq T_{C5} \\ E_r^5, & T_{C5} < T^* \end{cases} \quad (5)$$

where T_{C1} , T_{C2} , T_{C3} , T_{C4} and T_{C5} are the critical temperatures with the corresponding elastic modulus values E_r^1 , E_r^2 , E_r^3 , E_r^4 and E_r^5 , respectively. A_e and K_e are the exponential constants. The critical term T^* , which correlates the elastic modulus with cure degree, was represented as " $T^* = T - T_g$ " where T is the current temperature. During the DMA tests, the DOC was assumed to remain constant below T_g .

The five step CHILE model (Eq. (5)) was fitted to the elastic modulus measurements. The fitting was performed only in the temperature span of the tests, i.e. between 25°C and 200°C. A least squares non-linear regression analysis of the partial function was carried out in an in-house code which is based on 'fmincon' function in Matlab [43]. The critical temperatures were found via this analysis through the best fit for

Table 3
The estimated elastic modulus model parameters (Eq. (5)).

E_r^1 [MPa]	E_r^2 [MPa]	E_r^3 [MPa]	E_r^4 [MPa]	E_r^5 [MPa]	K_e [1/°C]
2446.0	2026.1	1406.7	352.6	12.3	0.1438
T_{C1} [°C]	T_{C2} [°C]	T_{C3} [°C]	T_{C4} [°C]	T_{C5} [°C]	A_e [MPa]
—	— 47.6	— 28.2	— 18.9	4.4	23.2947
122.9					

five samples with different DOC values. The calculated model constants are given in Table 3. The fitted model and the measured elastic modulus evolution are presented in Fig. 9(a). It is seen that the five step CHILE model captured the measured elastic modulus evolution as a function of temperature and DOC. Fig. 9(b) illustrates the predicted elastic modulus evolution for different DOC values ranging between 0.8 and 1.0.

5. Application on a typical pultrusion process

A case study was conducted to provide an insight about the material property evolution through a pultrusion line. A schematic of the pultrusion process and a representation of the material point that moves with the pulling speed of the profile are shown in Fig. 10(a). Here, the material point is defined as the point at which only the PU resin is present within the pultrusion die as indicated as "Case study region". The temperature profile presented in [28] was chosen to represent a typical pultrusion temperature profile within the pultrusion or heated die, i.e. "Case study region" seen in Fig. 10(a). The temperature was considered to be uniform throughout the cross section of the profile. This approximation is sufficiently valid for thin profiles as shown in [11]. A wide range of pulling speeds based on the temperature profile obtained from [28] for the pultrusion of PU resin was tested in the case study as shown in Fig. 10(b). The effect of pulling speeds on the evolution of DOC, viscosity and elastic modulus, was investigated by using the thermal histories given in Fig. 10(b) in the developed material models in this work. By using these material models, a process window or optimization can be achieved by analyzing the aforementioned material point. In this case study, the DOC, viscosity and elastic modulus evolution of the presented resin system were calculated inside the pultrusion die seen in Fig. 10(a). Although the reinforcement and sizing have effects on chemorheological and mechanical behaviour [44], in order to provide an understanding and description of the thermo-chemical mechanical behaviour of the pure PU resin, only the evolution of the resin properties through the process were considered in this case study.

Fig. 11 shows the cure degree, viscosity and elastic modulus

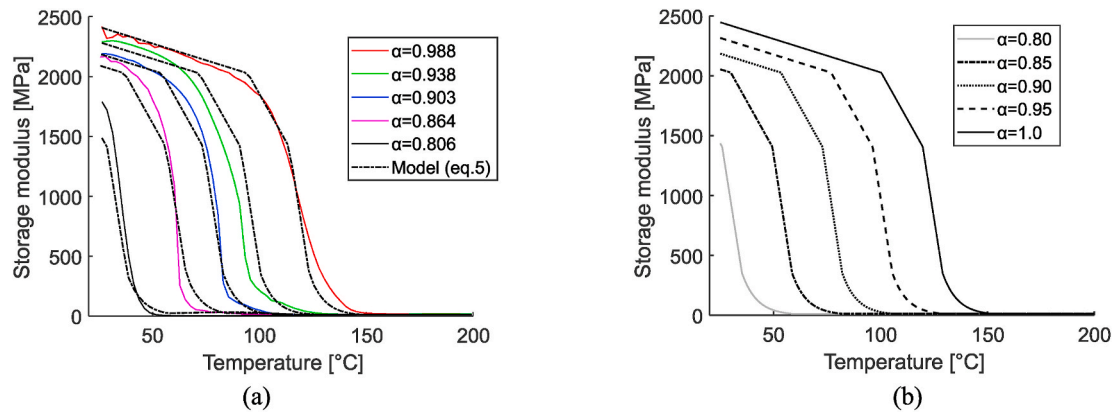


Fig. 9. Comparison of the measured and predicted elastic moduli (a). The predicted elastic moduli evolution at the corresponding cure degrees(b).

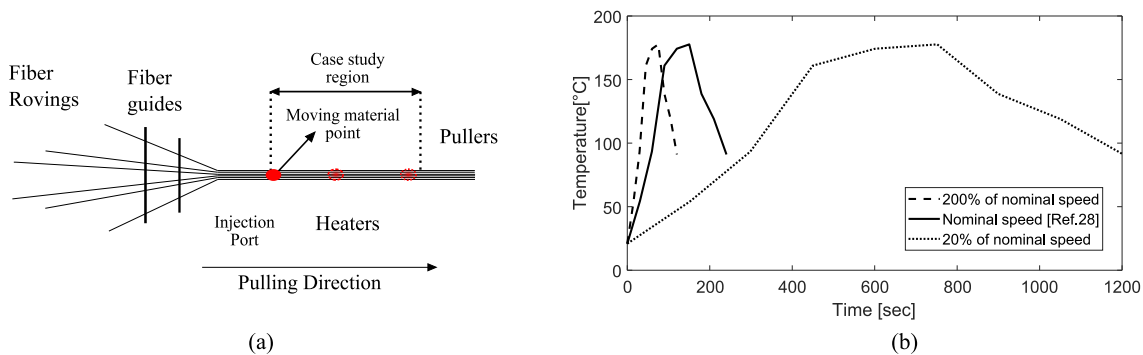


Fig. 10. A schematic representation of pultrusion process(a). Typical temperature profiles for pultrusion(b).

evolution through the die for various pulling speeds. As it is seen in Fig. 11(a), gelation occurs between 36% and 77% of the die length respectively for 20% and 200% of the nominal pulling speed. Therefore, the total length of rubbery phase within the die was different for different pulling speeds which in turn affects the pulling force [45]. In addition, the cure degree at the exit of die was found to be varying between 80.8% and 93.8% decreasing with increasing pulling speed. At the same time, the viscosity evolution affects the final product quality with respect to impregnation and void content [45]. The minimum viscosity predicted for the corresponding parameter set was $0.110 \text{ Pa} \cdot \text{s}$ which was observed at the 200% of nominal speed. On the contrary, for the 20% of pulling speed, the minimum predicted viscosity was $0.445 \text{ Pa} \cdot \text{s}$. The resultant cure degree would be a strong criterion for the final product's mechanical performance due to the cure degree dependency of elastic modulus. At the end of the die, the resin was in rubbery state for the pulling speeds higher than 50% of the nominal speed. For pulling speeds lower than 50% of the nominal speed, the profile exits the die in its glassy state. Still, the maximum elastic modulus observed in the die was below 1 GPa due to relatively high temperature. When the profile was assumed to be linearly cooled down to the room temperature within 2 min, the final elastic modulus varied from 1.55 GPa to 2.38 GPa as it is shown in Fig. 11(c).

6. Conclusion

A comprehensive material characterization study of a highly reactive PU resin system was carried out to capture the material behaviour in a pultrusion process model. The proposed constitutive material models, i. e. the cure kinetics and viscosity and elastic modulus, were fitted to the experimental results to predict the chemorheological and mechanical behaviour of a pultrusion specific PU system. The isothermal DSC tests were performed at 70°C , 90°C , 110°C , 120°C and 130°C . The dynamic

DSC scans were performed from 25°C to 200°C with a heating ramp of $5^\circ\text{C}/\text{min}$, $7.5^\circ\text{C}/\text{min}$ and $10^\circ\text{C}/\text{min}$. The average total heat of reaction was found to be approximately 275 J/g with a standard deviation of 8.3 J/g . The PU resin was approximately 80% cured within 160 s at 130°C .

Dynamic heating rates of $2.5^\circ\text{C}/\text{min}$, $5^\circ\text{C}/\text{min}$ and $7.5^\circ\text{C}/\text{min}$ were employed in the rheometer tests to obtain the complex viscosity evolution. The DOC at gelation was found to be approximately in the range of 0.75 and 0.79 for different heating rates.

A temperature sweep between 25°C and 200°C was carried out in the DMA tests for partially and fully cured PU resin. A cure degree and temperature dependent elastic modulus model was obtained by using a 5 step cure hardening instantaneous linear elastic model.

By using the developed material models, a case study was carried out to evaluate the effect of pulling speed on the evolution of material properties within the pultrusion die. The cure kinetics model, viscosity model and CHILE model can be used for numerical process models of similar two components polyurethane resin systems. Additionally, the experimental framework presented in this study can be utilized to characterize other types of fast curing thermoset resin systems.

To improve the data fitting procedure for determining the activation energy of the PU resin during curing, the consideration of different degree of cure values is reserved as a future work.

CRediT authorship contribution statement

Onur Yuksel: Conceptualization, Methodology, Software, Investigation, Visualization, Writing - original draft. **Michael Sandberg:** Validation, Writing - review & editing. **Ismet Baran:** Conceptualization, Software, Writing - review & editing, Supervision, Project administration, Funding acquisition. **Nuri Ersoy:** Writing - review & editing. **Jesper H. Hattel:** Writing - review & editing, Supervision, Project administration, Funding acquisition. **Remko Akkerman:** Supervision,

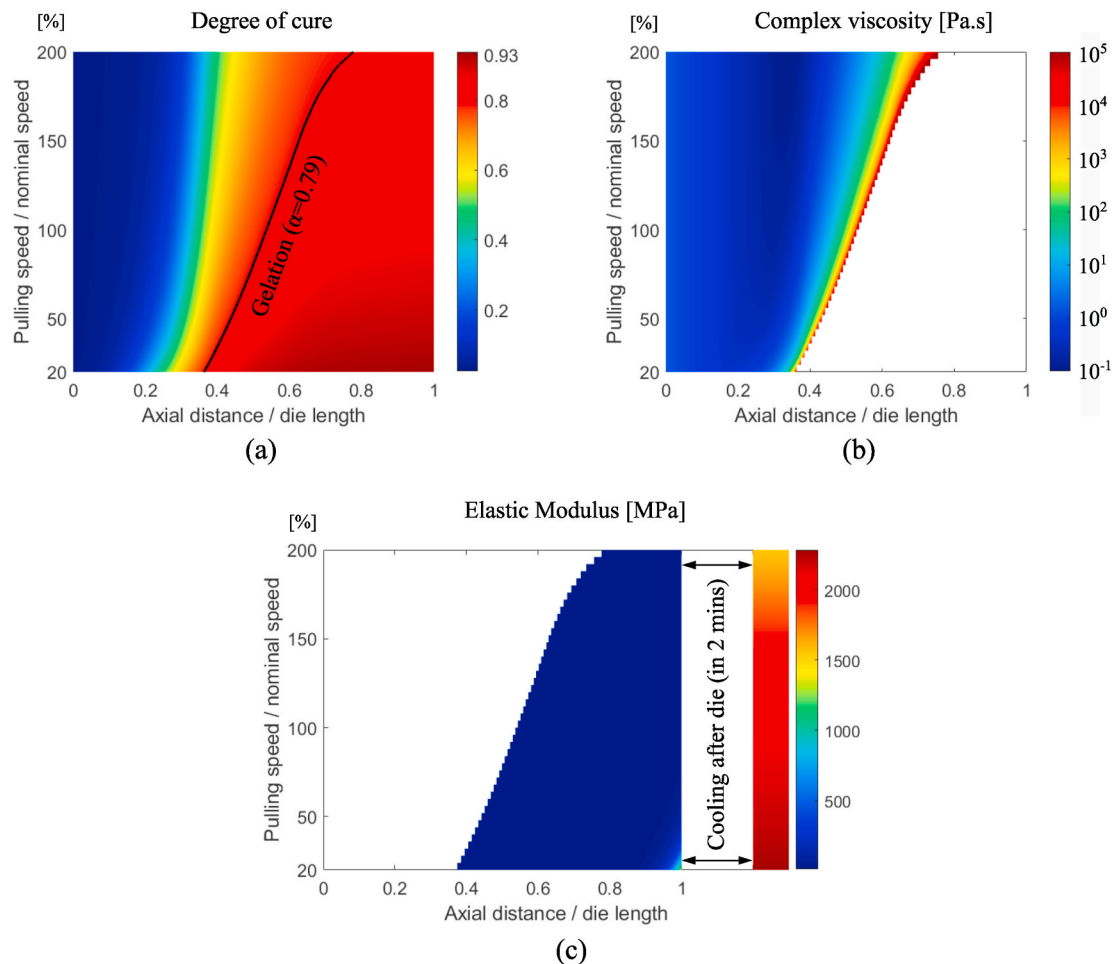


Fig. 11. Case study results; cure degree(a), viscosity(b) and elastic modulus(c) evolution within the die.

Project administration, Funding acquisition.

Declaration of competing interest

The authors declare that they have no known competing financial interests or personal relationships that could have appeared to influence the work reported in this paper.

Acknowledgements

This work is part of the project named ‘Modelling the multi-physics in resin injection pultrusion (RIP) of complex industrial profiles’ which has been granted by the Danish Council for Independent Research — Technology and Production Sciences (DFF /FTP), Grant no. DFF-6111-00112.

References

- [1] Starr T. Pultrusion for engineers. Taylor & Francis; 2000, ISBN 9780849308437.
- [2] Vedernikov A, Safonov A, Tucci F, Carlone P, Akhatov I. Pultruded materials and structures: a review. *J Compos Mater* 2020;54(26):4081–117.
- [3] Kennedy II K, Kusy R. Uv-cured pultrusion processing of glass-reinforced polymer composites. *J Vinyl Addit Technol* 1995;1(3):182–6.
- [4] Britnell D, Tucker N, Smith G, Wong S. Bent pultrusion - a method for the manufacture of pultrude with controlled variation in curvature. *J Mater Process Technol* 2003;138(1–3):311–5.
- [5] Silva F, Amorim E, Baptista A, Pinto G, Campilho R, Castro M. Producing hybrid pultruded structural products based on preforms. *Compos B Eng* 2017;116:325–32.
- [6] Irfan M, Shotton-Gale N, Paget M, Machavaram V, Leek C, Wootton S, et al. A modified pultrusion process. *J Compos Mater* 2017;51(13):1925–41.
- [7] Han C, Lee D, Chin H. Development of a mathematical model for the pultrusion process. *Polym Eng Sci* 1986;26(6):393–404.
- [8] Gadam S, Roux J, McCarty T, Vaughan J. The impact of pultrusion processing parameters on resin pressure rise inside a tapered cylindrical die for glass-fibre/epoxy composites. *Compos Sci Technol* 2000;60(6):945–58.
- [9] Simacek P, Advani S. Simulating tape resin infiltration during thermoset pultrusion process. *Compos Appl Sci Manuf* 2015;72:115–26.
- [10] Sandberg M, Rasmussen F, Hattel J, Spangenberg J. Simulation of resin-impregnation, heat-transfer and cure in a resin-injection pultrusion process. *AIP Conference Proceedings* 2019;2113(1):020022.
- [11] Baran I, Tutum C, Nielsen M, Hattel J. Process induced residual stresses and distortions in pultrusion. *Compos B Eng* 2013;51:148–61.
- [12] Baran I, Akkerman R, Hattel J. Modelling the pultrusion process of an industrial L-shaped composite profile. *Compos Struct* 2014;118:37–48.
- [13] Baran I, Hattel J, Akkerman R. Investigation of process induced warpage for pultrusion of a rectangular hollow profile. *Compos B Eng* 2015;68:365–74.
- [14] Baran I. Pultrusion: state-of-the-art process models. *Smithers Rapra*; 2015, ISBN 978-1910242421.
- [15] Khoun L, Centea T, Hubert P. Characterization methodology of thermoset resins for the processing of composite materials -Case study. *J Compos Mater* 2010;44(11):1397–415.
- [16] Baran I, Akkerman R, Hattel J. Material characterization of a polyester resin system for the pultrusion process. *Compos B Eng* 2014;64:194–201.
- [17] Michaeli W. Pultrusion of composite profiles-polyurethane (PU) as alternative matrix system. *Polym Polym Compos* 2010;18(9):537–42.
- [18] Engels H, Pirkel H, Albers R, Albach R, Krause J, Hoffmann A, et al. Polyurethanes: versatile materials and sustainable problem solvers for today's challenges. *Angew Chem Int Ed* 2013;52(36):9422–41.
- [19] Silva F, Baptista A, Pinto G, Campilho R, Ribeiro M. Characterization of hybrid pultruded structural products based on preforms. *Compos B Eng* 2018;140:16–26.
- [20] Monteavaro L, da Silva E, Costa A, Samios D, Gerbase A, Petzhold C. Polyurethane networks from formiated soy polyols: synthesis and mechanical characterization. *JAOCs (J Am Oil Chem Soc)* 2005;82(5):365–71.
- [21] Zlatanić A, Lava C, Zhang W, Petrović Z. Effect of structure on properties of polyols and polyurethanes based on different vegetable oils. *J Polym Sci B Polym Phys* 2004;42(5):809–19.
- [22] Sendjarevic I, Pietrzyk K, Schiffman C, Sendjarevic V, Kiziltas A, Mielewski D. Polyol from spent coffee grounds: performance in a model pour-in-place rigid polyurethane foam system. *J Cell Plast* 2020;0021955X20912204. 0(0).

- [23] Schneiderman D, Vanderlaan M, Mannion A, Panthani T, Batiste D, Wang J, et al. Chemically recyclable biobased polyurethanes. *ACS Macro Lett* 2016;5(4):515–8.
- [24] Yang W, Dong Q, Liu S, Xie H, Liu L, Li J. Recycling and disposal methods for polyurethane foam wastes. *Procedia Environmental Sciences* 2012;16:167–75.
- [25] Canal L, Benavente M, Hausmann M, Michaud V. Process-induced strains in rtm processing of polyurethane/carbon composites. *Compos Appl Sci Manuf* 2015;78: 264–73.
- [26] Mondragon I, de la Caba K, Stefani P, Rueda L, Eceiza A, d'Arlas BF. Kinetic and thermodynamic studies of the formation of a polyurethane based on 1,6-hexamethylene diisocyanate and poly(carbonate-co-ester)diol. *Thermochim Acta* 2007; 459(1–2):94–103.
- [27] Stanko M, Stommel M. Kinetic prediction of fast curing polyurethane resins by model-free isoconversional methods. *Polymers* 2018;10(7).
- [28] Prime RB, Michalski C, Neag CM. Kinetic analysis of a fast reacting thermoset system. *Thermochim Acta* 2005;429(2):213–7.
- [29] Kim D, Macosko C. Reaction kinetics and chemorheology of a highly reactive pu system. *Macromol Res* 1996;4(1):54–60.
- [30] Dimier F, Shirrazzuoli N, Vergnes B, Vincent M. Curing kinetics and chemorheological analysis of polyurethane formation. *Polym Eng Sci* 2004;44(3): 518–27.
- [31] Chiacchiarelli L, Kenny J, Torre L. *Thermochimica Acta* Kinetic and chemorheological modeling of the vitrification effect of highly reactive poly (urethane-isocyanurate) thermosets. *Thermochim Acta* 2013;574:88–97.
- [32] Zhang B, Duan H, Tao X, Dong W. Study on the mechanical properties of polyurethane based on ptmg-tmp system. *Polym Plast Technol Eng* 2018;57(17): 1743–51.
- [33] Keller A, Masania K, Taylor A, Dransfeld C. Fast-curing epoxy polymers with silica nanoparticles: properties and rheo-kinetic modelling. *J Mater Sci* 2016;51:236–51.
- [34] Connolly M, Heberer D. Advances in polyurethane pultrusion: cure modeling and 'second generation' resin systems. In: *COMPOSITES 2012- American composites manufacturers association ; conference date: 21-02-2011 through 23-02-2011*". Nevada USA: Las Vegas; 2011.
- [35] Johnston A. An integrated model of the development of process-induced deformation in autoclave processing of composite structures. Ph.D. thesis; University of British Columbia; 1997.
- [36] Mezger T. The rheology handbook. *Coatings compendia*. Elsevier Science Limited; 2006, ISBN 9780815515296.
- [37] Lucio B, de la Fuente J. Rheological cure characterization of an advanced functional polyurethane. *Thermochim Acta* 2014;596:6–13.
- [38] de la Caba K, Guerrero P, Eceiza A, Mondragon I. Kinetic and rheological studies of an unsaturated polyester cured with different catalyst amounts. *Polymer* 1996;37 (2):275–80.
- [39] Castro J, Macosko C. Studies of mold filling and curing in the reaction injection molding process. *AIChE J* 1982;28(2):250–60.
- [40] Nielsen LE. Cross-linking-effect on physical properties of polymers. *J Macromol Sci, Part C* 1969;3(1):69–103.
- [41] DiBenedetto AT. Prediction of the glass transition temperature of polymers: a model based on the principle of corresponding states. *J Polym Sci B Polym Phys* 1987;25(9):1949–69.
- [42] Pascault JP, Williams RJJ. Glass transition temperature versus conversion relationships for thermosetting polymers. *J Polym Sci B Polym Phys* 1990;28(1): 85–95.
- [43] MATLAB version 9.7.0.1216025 (R2019b) Update 1. Natick, Massachusetts: The Mathworks, Inc.; 2019.
- [44] Thomason J. Glass fibre sizing: a review. *Compos Appl Sci Manuf* 2019;127: 105619.
- [45] Carlone P, Baran I, Hattel J, Palazzo G. Computational approaches for modeling the multiphysics in pultrusion process. *Adv Mech Eng* 2013;5.